PHYSICAL REVIEW C VOLUME 22, NUMBER 5 NOVEMBER 1980

Comprehensive relations for hadron-nucleus inelastic excitations in terms of elastic scattering

R. D. Amado
Department of Physics, University of Pennsylvania, Philadelphia, Pennsylvania 19104

F. Lenz*
Department of Physics, Massachusetts Institute of Technology, Cambridge, Massachusetts 02139

J. A. McNeil and D. A. Sparrow
Department of Physics, University of Pennsylvania, Philadelphia, Pennsylvania 19104
(Received 26 February 1980)

We obtain closed form asymptotic approximations to the eikonal form for inelastic hadron-nucleus scattering to strongly excited nuclear states. These forms exploit the dominance of the nuclear geometry recently used by us to obtain the elastic scattering amplitudes. Our forms agree well with the data. We find that the inelastic scattering can be written in terms of the elastic scattering cross section. These data-to-data forms agree remarkably well with experiment and serve to emphasize the geometric unity of the reactions. The simplicity of these expressions and relations should make them useful in medium energy phenomenology.

[NUCLEAR REACTIONS Closed form eikonal amplitude for hadron-nucleus inelastic scattering. Data-to-data form relating inelastic and elastic scattering.]

I. INTRODUCTION

Hadron-nucleus scattering at intermediate energies has been extensively studied experimentally and well fitted theoretically by numerical calculations. For elastic scattering treated in the eikonal approximation, we have recently shown[1] that these fits can be understood *analytically* by exploiting the dominance of nuclear geometry in the scattering mechanism. In this paper we extend these analytic methods to the inelastic scattering of hadronic probes to strongly excited nuclear states. We again find simple analytic results by exploiting the geometry of the nucleus as manifested in the eikonal approximation. As an added bonus we find that the cross section for inelastic scattering can be expressed directly in terms of the cross section for elastic scattering. These data-to-data formulas work remarkably well when applied to experiment. All these results serve to emphasize the basic geometric nature of these reactions and, correspondingly, the relative insensitivity to dynamics for strong inelastic scattering. The data-to-data formulas provide a remarkably simple phenomenological tool for relating elastic and inelastic scattering, and underline the unity of these processes by organizing them into a single comprehensive picture. The data-to-data formulas are in some sense better than the derivation used to obtain them since they automatically correct for parts neglected in the derivation (e.g., Coulomb interaction). Furthermore, they ensure that the sensitive details of reaction dynamics, such as minimum filling, are correctly accounted for in comparing elastic and inelastic processes without requiring a microscopic theory of them. The remaining dependence on nuclear shape parameters needed to make the data-to-data comparisons is mild.

For inelastic scattering, the major assumption of our work is a local, surface peaked transition density. We embed this in a distorted wave impulse approximation with eikonal treatment of the distortion and use the stationary phase methods we developed for elastic scattering to evaluate the integral. The surface peaked transition density (Tassie[2] model) is a good approximation for collective states, which are also the states that are strongly excited. For inealstic proton scattering at medium energy, strong refraction at the surface and strong absorption tend to favor surface excitation even if the transition density does not. That is one of the reasons for the empirical success of the Tassie form for (p,p') reactions. To test truly the excitation mechanism one should study a less strongly absorbed or refracted probe. For processes involving two-step excitation, for example intermediate resonance formation, our locality assumption presumably fails. Such processes therefore give hope of shedding some light

on the details of the dynamics, in spite of the fact that they often correspond to relatively weak cross sections.

In Sec. II we obtain the formulas for inelastic scattering. We do this by beginning with the excitation of low spin collective states, which is somewhat simpler, and then proceed to the general case. The reader interested only in the answer should skip to Eq. (2.51) for the data-to-data formula. Section III contains comparison with results primarily for (p,p') reactions. Agreement is excellent. Section IV concludes with some general discussion and points for further study. Two technical points are dealt with in the Appendices.

II. THEORY OF INELASTIC SCATTERING

Consider the inelastic scattering at intermediate energy of a hadron (e.g., proton, but we neglect spin) from a nuclear target to a particular target state. We take the target ground state to have spin zero and the excited state to be an L^π state. It is well known that excitations of discrete states are well understood in terms of the distorted wave impulse approximation. The distorted waves may be generated using either the Schrödinger equation or an eikonal formalism. Neglecting any difference in distortion between the ground and excited states, the scattering amplitude for the process can be written

$$\langle \vec{p}' L^\pi M | A | \vec{p} 0^+ \rangle = \frac{ip}{2\pi} \int \psi^*_{\vec{p}'}(\vec{r}) \langle \vec{r} L^\pi M | V_t | \vec{r} 0^+ \rangle \times \psi_{\vec{p}}(\vec{r}) d^3 r . \tag{2.1}$$

We have called the incident and final center of mass momenta of the projectile $\vec{p}$ and $\vec{p}'$ respectively, and have assumed that the transition density V_t is local. M is the projection of the final state target angular momentum. We use eikonal wave functions for the distorted waves ψ, obtaining

$$\langle \vec{p}' L^\pi M | A | \vec{p} 0^+ \rangle = \frac{ip}{2\pi} \int d^3 r , e^{i\vec{q}\cdot\vec{r}} e^{-\chi(b)} \times \langle \vec{r} L^\pi M | V_t | \vec{r} 0^+ \rangle \tag{2.2}$$

where $\vec{q} = \vec{p} - \vec{p}'$ is the momentum transfer. At intermediate energies we can use the first order local density form for the eikonal profile function $\chi(b)$:

$$\chi(b) = \gamma t(b) , \tag{2.3a}$$

$$t(b) = \int_{-\infty}^{\infty} \rho[(z^2 + b^2)^{1/2}] dz , \tag{2.3b}$$

where ρ is the nuclear density normalized to $\int \rho(r) d^3 r = A$, and z is the incident direction so that $\vec{b}$ is a two-vector in the impact parameter plane. γ is defined by

$$\gamma = \tfrac{1}{2} \sigma_{\text{tot}} (1 - ir) , \tag{2.4}$$

where σ_{tot} is the total cross section and r is the ratio of real to imaginary part of the forward amplitude for projectile-nucleon scattering. At small angles, $\vec{q}$ has a significant component only in the $\vec{b}$ plane so we can write $\vec{q}\cdot\vec{r} \cong \vec{q}\cdot\vec{b} = qb\cos\phi$. On general invariance grounds we may write for the transition density

$$\langle \vec{r} L^\pi M | V_t | \vec{r} 0^+ \rangle = f_L(r) Y_{L,M}(\theta, \phi) = f_L(r) P_{L,M}(\theta) e^{iM\phi} , \tag{2.5}$$

where in the last step we have written the spherical harmonic in terms of the associate Legendre polynomial P_{LM}. The amplitudes corresponding to $\pm M$ can differ by at most a phase, so to calculate cross sections we need only consider $M \geq 0$. Inserting (2.5) in (2.2) and using the integral representation of the Bessel function, we can evaluate the ϕ integral to obtain

$$\langle \vec{p}' L^\pi M | A | \vec{p} 0^+ \rangle = ip \int_0^\infty J_M(qb) b\, db\, e^{-\chi(b)} \times \int_{-\infty}^{\infty} dz f_L(r) P_{L,M}(\theta) \times i^{-m} , \tag{2.6}$$

where in the last integral we must recall that $r^2 = b^2 + z^2$ and that P_{LM} is a homogeneous polynomial in $b^{L-n} z^n r^{-L}$. The powers n are odd if $L+M$ is odd and even if $L+M$ is even. Therefore the z integral in (2.6) will vanish unless $L+M$ is even. Apart from the standard assumptions of the distorted wave eikonal approximation, and the assumption that the transition density is local, Eq. (2.6) is completely general.

We now specialize to the case of excitation of collective transitions. It is well known that for such cases the transition density is strongly peaked at the nuclear surface. Of course, even if it were not, the absorption and refraction due to $\chi(b)$ would force most of the transition strength to act at the surface. We will return to this point. For collective transitions, it is convenient to parametrize f_L in the form (Tassie[2])

$$f_L(r) = \lambda_L r^L \frac{1}{r}\frac{d}{dr} \rho(r) , \tag{2.7}$$

where λ_L is a parameter describing the excitation strength and ρ is the same nuclear density as in (2.3). Using (2.7) in (2.6) gives an excellent account of the data for the inelastic excitation of collective states of medium and large nuclei at intermediate energies. Normally this agreement

is obtained via numerical evaluation of (2.6) with (2.7) after careful numerical adjustment of the eikonal parameters to fit the elastic scattering, also calculated numerically. We will now show that this agreement is no surprise since the inelastic cross section obtained from (2.6) and (2.7) can be expressed directly in terms of the elastic cross section.

Let us begin with the case of a 1^- state since it is a particularly simple example, even though it seems to be of little empirical interest. Because of the rule that $L+M$ must be even, we need only study $L=1$, $M=1$, and have $P_{1,1}=-(3/8\pi)^{1/2}b/r$. Calling the amplitude $A_{1,1}$, we have

$$A_{1,1}=-p\lambda_1\left(\frac{3}{8\pi}\right)^{1/2}\int_0^\infty b^2db\,J_1(qb)e^{-\chi(b)} \times\int_{-\infty}^{\infty}dz\,\frac{1}{r}\frac{d}{dr}\rho(r)\,. \quad (2.8)$$

Using $(1/r)(d/dr)\rho=(1/z)(d/dz)\rho$ from $r^2=b^2+z^2$ and (2.3), this becomes

$$A_{1,1}=-p\lambda_1\left(\frac{3}{8\pi}\right)^{1/2}\int_0^\infty b\,db\,J_1(qb)e^{-\chi(b)}\frac{1}{\gamma}\frac{d}{db}\chi(b)\,, \quad (2.9)$$

which can be written

$$A_{1,1}=-p\,\frac{\lambda_1}{\gamma}\left(\frac{3}{8\pi}\right)^{1/2}\int_0^\infty b\,db\,J_1(qb)\frac{d}{db}(1-e^{-\chi(b)})\,. \quad (2.10)$$

If we integrate by parts, note that the boundary terms are zero [$\chi(\infty)=0$], and use the Bessel function identity

$$\frac{d}{db}bJ_1(qb)=qbJ_0(qb)\,, \quad (2.11)$$

we obtain

$$A_{1,1}=p\,\frac{\lambda_1}{\gamma}\left(\frac{3}{8\pi}\right)^{1/2}q\int_0^\infty b\,db\,J_0(qb)(1-e^{-\chi(b)}) =-i\,\frac{\lambda_1}{\gamma}\left(\frac{3}{8\pi}\right)^{1/2}qA_0\,, \quad (2.12)$$

where A_0 is the hadron-nucleus elastic scattering amplitude in the eikonal approximation. For the inelastic cross section we have

$$\sigma_{\text{in},1^-}=|A_{1,1}|^2+|A_{1,-1}|^2=\left|\frac{\lambda_1}{\gamma}\right|^2\frac{3}{4\pi}q^2\sigma_{\text{el}}\,. \quad (2.13)$$

By making the additional assumptions that the inelastic transition is driven by the same part of the hadron-nucleon force as the elastic scattering, and further that the excitation is of $T=0$ character, λ_1 may be written in terms of γ and the reduced electromagnetic rate (see Appendix B),

$$\lambda_1=\gamma[\tfrac{1}{3}B(E1)\uparrow]^{1/2}\frac{4\pi}{3Z}\,. \quad (2.14)$$

In Eq. (2.14) Z is the nuclear charge. Finally, the cross section for the inelastic excitation of a 1^- collective state is given by

$$\sigma_{\text{in},1^-}(q)=q^2\,\frac{B(E1)\uparrow}{4\pi}\left(\frac{4\pi}{3Z}\right)^2\sigma_{\text{el}}(q)\,. \quad (2.15)$$

Equation (2.13) is the archetype of relations we will obtain for other values of L. It expresses $\sigma_{\text{in},L}$ directly in terms of σ_{el} and λ_L. We will find the factor of q^2 for all transitions, but for higher L we will find a shift in the q at which $\sigma_{\text{in},L}$ and σ_{el} are to be compared. We will also find that the result cannot be obtained without making more detailed assumptions about the elastic eikonal amplitude. Fortunately we have recently obtained considerable insight into the form of that amplitude that will enable us to do just that.[1]

Let us turn to the case of $L=2$. There are two M values that satisfy $M+L$ even, $M=2$ or 0. Since $P_{2,2}=(15/32\pi)^{1/2}b^2/r^2$, we have for the amplitude $A_{2,2}$

$$A_{2,2}=-ip\lambda_2\left(\frac{15}{32\pi}\right)^{1/2}\int_0^\infty b^3db\,J_2(qb)e^{-\chi(b)} \times\int_{-\infty}^{\infty}dz\,\frac{1}{r}\frac{d}{dr}\rho(r)\,. \quad (2.16)$$

Following the procedure we used to go from Eq. (2.8) to (2.10) and integrating by parts we obtain

$$A_{2,2}=ip\,\frac{\lambda_2}{\gamma}\left(\frac{15}{32\pi}\right)^{1/2}\int_0^\infty db\,\frac{d}{db}[b^2J_2(qb)] \times(1-e^{-\chi(b)})\,. \quad (2.17)$$

Now using the Bessel function identities

$$\frac{d}{db}[b^2J_2(qb)]=qb^2J_1(qb)=-q\,\frac{d}{dq}bJ_0(qb)\,, \quad (2.18)$$

we obtain

$$A_{2,2}=-\,\frac{\lambda_2}{\gamma}\left(\frac{15}{32\pi}\right)^{1/2}q\,\frac{d}{dq}A_0\,. \quad (2.19)$$

For the case of $M=0$ we use $P_{2,0}=(5/16\pi)^{1/2}(2z^2-b^2)/r^2$. In (2.6) we must study

$$\int_{-\infty}^{\infty}dz(2z^2-b^2)\,\frac{1}{r}\frac{d}{dr}\rho(r)\,. \quad (2.20)$$

Using $(1/r)(d/dr)\rho=(1/z)(d/dz)\rho$ in the z^2 term and integrating by parts, we find for (2.20)

$$-b\,\frac{d}{db}t(b)-2t(b)\,. \quad (2.21)$$

The inelastic amplitude is therefore

$$A_{2,0}=-ip\left(\frac{5}{16\pi}\right)^{1/2}\lambda_2\int_0^\infty b\,db\,J_0(qb)e^{-\chi(b)}\times\left(b\frac{d}{db}+2\right)t(b)\,. \quad (2.22)$$

Using $t(b)=-(d/d\gamma)e^{-\chi(b)}$ and integrating by parts for the b derivative, we obtain

$$A_{2,0}=\left(\frac{5}{16\pi}\right)^{1/2}\frac{\lambda_2}{\gamma}\left(q\frac{d}{dq}+2-2\gamma\frac{d}{d\gamma}\right)A_0\,. \quad (2.23)$$

In order to make further progress in using (2.19) or (2.23) we need to have an explicit formula for A_0 that we can differentiate with respect to q and γ. For that we turn to our recent work on an explicit formula for hadron-nucleus elastic scattering in the eikonal approximation.[1] We have shown that the integral for A_0 can be evaluated to a very good approximation using the asymptotic form of the Bessel function and the method of stationary phase. Our approximate form for A_0 yields a cross section that agrees essentially perfectly with exact numerical evaluation except at the smallest values of q. We now turn to the form. We write following Ref. 1, hereafter referred to as ADL,

$$A_0(q,p)=-ip[G(q,\gamma)+G^*(q,\gamma^*)]\,. \quad (2.24)$$

The leading asymptotic approximation to G, G_s, is given by [ADL Eq. (40)]

$$G_s(q,\gamma)=\frac{\alpha^{1/3}b_0^{2/3}q^{-4/3}}{\sqrt{3}}\exp[\tfrac{5}{6}\pi i-\gamma\tilde{t}(b_0)+iqb_0+\tfrac{3}{2}(\alpha^2qb_0)^{1/3}e^{i\pi/6}], \quad (2.25)$$

where $b_0=c+i\pi\beta$ with c the nuclear radius and β the skin thickness parameter appropriate to a Fermi distribution

$$\rho(r)=\rho_0\left[1+\exp\left(\frac{r-c}{\beta}\right)\right]^{-1} \quad (2.26)$$

and $\alpha=2\pi\gamma\beta\rho_0$ is a dimensionless "strength" parameter. $\tilde{t}$ is the nonsingular part of the profile function defined as in (2.3b) but using $\tilde{\rho}$ where

$$\tilde{\rho}(r)=\rho(r)+2b_0\beta\rho_0/(r^2-b_0^2)\,. \quad (2.27)$$

The G_s of (2.25) contains only the leading asymptotic contributions and does not include the effect of the Coulomb interaction. In fact, ADL also gives a closed form expression for G with first order nonasymptotic correction and the Coulomb interaction included [ADL (57)], but we will use the algebraically simpler form (2.25) for our discussion. Given (2.24) and (2.25) it is straightforward to calculate $A_{2,0}$ and $A_{2,2}$. The general form of $A_{2,0}$ is rather complicated and we can take advantage of the structure of G_s to greatly simplify it. Most of the q dependence of (2.25) comes from the term $\exp(iqb_0)$. In fact, as pointed out in ADL, for reasonable choices of parameters in proton nucleus scattering the remaining q dependence largely cancels between the $q^{-4/3}$ term and the $q^{1/3}$ term in the exponent. Therefore $q(d/dq)G_s=iqb_0G_s$ is a very good approximation. In most of the scattering region $|qb_0|\gg1$, since the γ derivative in A_0 brings down a factor of order $(qb_0)^{1/3}$ and the other factor is 2, the q derivative term dominates. Therefore $A_{2,0}$ becomes proportional to $A_{2,2}$ for $|qb_0|\approx qc\gg1$. We have for $A_{2,2}$

$$A_{2,2}\cong-ip\,\frac{\lambda_2}{\gamma}\left(\frac{15}{32\pi}\right)^{1/2}q[ib_0G_s(q,\gamma)-ib_0^*G_s^*(q,\gamma^*)] \quad (2.28)$$

and for $A_{2,0}$

$$A_{2,0}=(\tfrac{2}{3})^{1/2}A_{2,2}\,. \quad (2.29)$$

If we write

$$b_0=B_0e^{i\phi}\,, \quad (2.30)$$

where B_0 is the magnitude of b_0, then

$$A_{2,2}=-ip\,\frac{\lambda_2}{\gamma}\left(\frac{15}{32\pi}\right)^{1/2}qB_0[e^{i(\phi+\pi/2)}G_s(q,\gamma)+e^{-i(\phi+\pi/2)}G_s^*(q,\gamma^*)]\,. \quad (2.31)$$

Thus $\phi+\pi/2$ is just a phase shift in the oscillations of G. Those oscillations are controlled by the imaginary part of the iqb_0 factor, which is iqc. The real part of this factor contributes an exponential decrease of the amplitude of $e^{-\pi\beta}$. As stressed above, these are the most significant contributions to the q dependence. Thus we can express $A_{2,2}$ at q in terms of A_0 at $q+(\phi+\pi/2)c$, however we must remove the scale shift due to the exponential factor. We find

$$A_{2,2}\cong-\frac{\lambda_2}{\gamma}\left(\frac{15}{32\pi}\right)^{1/2}qB_0A_0\left[q+\left(\phi+\frac{\pi}{2}\right)\Big/c,p\right]\times\exp\left[\pi\beta\left(\phi+\frac{\pi}{2}\right)\Big/c\right]. \quad (2.32)$$

Using (2.29) between $A_{2,2}$ and $A_{2,0}$ we can write for the cross section

$$\sigma_{\text{in},2^+}(q)=\left|\frac{\lambda_2}{\gamma}\right|^2\frac{5}{4\pi}(qB_0)^2\exp\left[\left(\frac{2\pi\beta}{c}\right)\left(\phi+\frac{\pi}{2}\right)\right]\times\sigma_{\text{el}}\left[q+\left(\phi+\frac{\pi}{2}\right)\Big/c\right]. \quad (2.33)$$

For small scattering angle θ and high energy we

can neglect the excitation energy contribution to the momentum transfer and have

$$q \cong p\theta , \tag{2.34}$$

so that (2.33) relates $\sigma_{\text{in},2}$ at θ to σ_{el} at $\theta + (\phi + \pi/2)/pc$. We shall see in Sec. IV that this data-to-data comparison is remarkably accurate.

For $L = 3^-$, we must consider $M = 1$ and 3. We write the inelastic version of (2.24)

$$A_{3,M} = ip[G_{s,3M}(q, \gamma) + G^*_{s,3M}(q, \gamma^*)] . \tag{2.35}$$

Using explicit forms for $P_{3,3}$ and $P_{3,1}$, and the by now familiar tricks of integration by parts and Bessel function identities, we find that $G_{s,3M}$ can be expressed in terms of the elastic G_s and its derivatives, except that we find more powers of b in the integrand. In ADL we emphasized that in evaluating the b integral the complex singularity of $\chi(b)$ at $b = b_0$ dominates, so that we can evaluate all polynomials in b at $b = b_0$. Doing this we find

$$G_{s,31}(q, \gamma) = i \frac{\lambda_3}{4\gamma}\left(\frac{21}{4\pi}\right)^{1/2} q\left(b_0^2 - \frac{2}{q}\frac{d}{dq} + \frac{4\gamma}{q}\frac{d}{d\gamma}\frac{d}{dq}\right) \times G_s(q, \gamma) \tag{2.36}$$

and

$$G_{s,33}(q, \gamma) = -i \frac{\lambda_3}{4\gamma}\left(\frac{35}{4\pi}\right)^{1/2} q\left(b_0^2 + \frac{2}{q}\frac{d}{dq}\right) G_s(q, \gamma) . \tag{2.37}$$

Again, for large qc the first term in the brackets in (2.36) and (2.37) dominates and we have $G_{s,31} \sim G_{s,33}$. Using (2.30) this gives for (2.35)

$$A_{3,M} \cong ip \frac{\lambda_3}{4\gamma}\left(\frac{n_M}{4\pi}\right)^{1/2} qB_0^2[G_s(q, \gamma)e^{2i\phi} + G^*_s(q, \gamma^*)e^{-2i\phi}] \times i^{-m} , \tag{2.38}$$

where $n_1 = 21$ and $n_3 = 35$. We obtain for the inelastic cross section

$$\sigma_{\text{in},3}(q) = \left|\frac{\lambda_3}{\gamma}\right|^2 \frac{7}{4\pi} B_0^2 (qB_0)^2 e^{4\pi\beta\phi/c}\sigma_{\text{el}}(q + 2\phi/c), \tag{2.39}$$

or using (2.34) to simplify the expression in terms of θ,

$$\sigma_{\text{in},3}(\theta) = \left|\frac{\lambda_3}{\gamma}\right|^2 \frac{7}{4\pi} B_0^2 (qB_0)^2 \times e^{4\pi\beta\phi/c}\sigma_{\text{el}}(\theta + 2\phi/pc) , \tag{2.40}$$

which is a data-to-data formula for the 3^- excitation and, as we shall see in Sec. IV, works remarkably well.

For general L and $L + M$ even, P_{LM} can be written

$$P_{L,M} = r^{-L} \sum_n a_n b^{L-2n} z^{2n} \tag{2.41}$$

with upper limit $L/2$ or $(L-1)/2$ depending on whether L is even or odd. Substituting in (2.6) with (2.7), we have

$$A_{L,M} = ip\lambda_L \sum_n \int_0^\infty db\, b^{L-2n+1} J_M(qb) e^{-\chi(b)} \times \int_{-\infty}^{\infty} z^{2n} dz \frac{1}{r}\frac{d}{dr}\rho(r) \times i^{-m} . \tag{2.42}$$

The factor $e^{-\chi(b)}$ by penetrability and refraction will tend to favor large values of b which, because of the localized density, implies small z. The leading contribution to (2.42), therefore, comes from $n = 0$. We show in Appendix A that the $n \neq 0$ terms are down by $(qb_0)^{-2/3}$ and powers of it. This neglect of terms in z is precisely the argument we used to get to Eq. (2.29) or from (2.36) and (2.37) to (2.38). Keeping only the $n = 0$ term, we have

$$\begin{aligned} A_{L,M} &= ip\lambda_L a_0 \int_0^\infty db\, b^{L+1} J_M(qb) e^{-\chi(b)} \frac{1}{b}\frac{d}{db} \times \int_{-\infty}^{\infty} \rho(r)\, dz \cdot i^{-m} \\ &= -ip\lambda_L a_0 \int_0^\infty db \frac{d}{db}[b^L J_M(qb)] \times (1 - e^{-\chi(b)}) \cdot i^{-m} , \end{aligned} \tag{2.43}$$

where in the last step we have done the usual steps including integration by parts. We now separate (2.43) as in (2.35) using $J_M(x) = \frac{1}{2}[H^{(1)}_M(x) + H^{(2)}_M(x)]$ and $H^{(1)}_M(x) = H^{(2)}_M(x)^*$, giving

$$A_{L,M} = ip[G_{L,M}(q, \gamma) + G^*_{L,M}(q, \gamma^*)] , \tag{2.44}$$

where

$$G_{L,M}(q, \gamma) = -\frac{\lambda_L}{2\gamma} a_0 \int_0^\infty db \frac{d}{db}[b^L H^{(1)}_M(qb)] \times (1 - e^{-\chi(b)}) . \tag{2.45}$$

For large qb we can use the asymptotic expansion of $H^{(1)}_M$, $H^{(1)}_M(x) \sim (2/\pi x)^{1/2} \exp i(x - \pi M/2 - \pi/4)$, and obtain

$$G_{L,M}(q,\gamma) \cong -\frac{\lambda_L}{2\gamma} a_0 e^{-i[(\pi/2)M+\pi/4]} \times \int_0^\infty db \frac{d}{db}\left[b^L\left(\frac{2}{\pi q b}\right)^{1/2} e^{iqb}\right] \times (1-e^{-\chi(b)}). \quad (2.46)$$

Again for large q the derivative of the exponential factor dominates and the integral for G_{LM} becomes just the same as the integral for the elastic G except for the factor of b^{L-1} (one power of b combines with db in the integration measure). Evaluating the integral as in ADL by deforming the contour and exploiting the singularity of $\chi(b)$ at $b=b_0$ so that all polynomial factors and other slowly varying factors can be evaluated at $b=b_0$, we can express G_{LM} asymptotically ($G_{s,LM}$) in terms of G_s of (2.25).

$$G_{s,LM} = -\frac{\lambda_L}{\gamma} a_0 e^{-i\pi M/2} i q b_0^{L-1} G_s(q,\gamma). \quad (2.47)$$

Note that (2.36) and (2.37) are special cases of this formula. Recall that for L odd (even) M is odd (even) and that only the relative phase of G_{LM} and G_{LM}^* matter in constructing a cross section from (2.44). Using (2.30) we can write (up to an unobservable overall phase)

$$A_{L,M} = ip\frac{\lambda_L}{\gamma} a_0 q B_0^{L-1} \times (\exp\{i[(L-1)\phi+\eta]\} G_s(q,\gamma) + \exp\{-i[(L-1)\phi+\eta]\} G_s^*(q,\gamma^*)), \quad (2.48)$$

where $\eta=0$ if L is odd and $\eta=\pi/2$ if L is even. To construct the inelastic cross section for (2.48) we need the sum $\sum |a_0|^2$ over the appropriate odd or even M values. It can be shown from the definition in (2.41) that

$$\sum |a_0|^2 = \frac{2L+1}{4\pi}. \quad (2.49)$$

Putting it all together we have the generalization of (2.40)

$$\sigma_{\text{in},L}(q) = \left|\frac{\lambda_L}{\gamma}\right|^2 \frac{2L+1}{4\pi} B_0^{2(L-2)} (qB_0)^2 \times \exp(2\pi\beta\Phi_L/c)\sigma_{el}(q+\Phi_L/c), \quad (2.50)$$

where $\Phi_L = (L-1)\phi + \eta$ (2.30) and $\eta=0$ for odd L and $\pi/2$ for even L. Using (2.34) we can write

$$\sigma_{\text{in},L}(\theta) = \left|\frac{\lambda_L}{\gamma}\right|^2 \frac{2L+1}{4\pi} B_0^{2(L-2)} (qB_0)^2 \times \exp(2\pi\beta\Phi_L/c)\sigma_{el}(\theta+\Phi_L/pc). \quad (2.51)$$

This is our general result. It relates the inelastic cross section for excitation of a collective state of spin L at angle θ to the cross section for elastic scattering at the angle $\theta+\Phi_L/pc$ in terms of purely kinematic factors and the overall strength of the excitation $|\lambda_L|^2$.

It is customary to relate the magnitudes of inelastic hadron cross sections to the appropriate $B(EL)$'s whenever possible. We have avoided this thus far (except for the 1^- case) since specification of the normalization relative to a $B(EL)$ in general, requires detailed knowledge of the nuclear interior. For a 1^- excitation of a $T=0$ nature the normalization is absolute with no further assumptions about the density, because the radial integral involved in computing the $B(E1)$ can be related to the density normalization integral. For higher L values the normalization of the $B(EL)$ is not so simply computed and the relation between the normalization of the inelastic cross section and the electromagnetic rates will depend on the details of the functional form of the density and on the relative contributions of neutrons and protons to the inelastic process. Rather than become enmeshed in these details, we have generally chosen to normalize our results via the parameter λ_L. However, if we assume that the transition is driven by the same part of the force that drives elastic scattering, and that neutrons and protons contribute equally ($\Delta T=0$ transition), we obtain

$$\lambda_L = \frac{4\pi\gamma[B(EL)]^{1/2}}{3Z\int_0^\infty dr\, r^{2l+2}\rho(r)} \quad (2.52)$$

or

$$\left|\frac{\lambda_L}{\gamma}\right|^2 = \left(\frac{4\pi}{3Z}\right)^2 \frac{B(EL)}{\int_0^\infty dr\, r^{2l+2}\rho(r)}. \quad (2.53)$$

In Eqs. (2.52) and (2.53) the density that appears is the ground state density. Again, it should be stressed that the uncertainties associated with the interior affect the $B(EL)$ rather than the hadron scattering. We may nevertheless use this to obtain an absolutely normalized expression. This expression is worked out for a Fermi ground state distribution in Appendix B. The constant relating λ_L and the $B(EL)$ may depend strongly on the form of the density. However, Eqs. (2.52) and (2.53) depend only on the assumption of a Tassie relationship between the ground state and transition densities.

Finally we note that our data-to-data form (2.51) is not only surprisingly simple, but also quite general. For example, we obtain the Blair[3] phase rule in the special case of a sharp edge for the nucleus.[4] For electron excitation there is the same shift between elastic and inelastic scattering as in (2.51). We plan to return to a complete treatment of the electron problem. As we shall see in Sec. III, the simple data-to-data result works re-

markably well. In particular, the formula is *better* than the steps used to derive it since by comparing data to data it corrects for slowly varying mistakes in how (2.25) deals with the elastic scattering, for example, in the assumptions about nuclear geometry and the neglect of the Coulomb interaction. Of course in the derivation of (2.51) we used qc large, and therefore it will not work for forward scattering, where threshold effects are important.

III. RESULTS AND COMPARISON WITH DATA

In Sec. II we showed that the expressions for inelastic scattering cross sections of hadrons from nuclei at medium energy in the eikonal approximation can be manipulated into simple analytic formulas by which these quantities can be related to corresponding elastic scattering cross sections. In this section we test these analytic approximate forms against the full numerical results and test the relationship between elastic scattering data and inelastic scattering data. It is not our major purpose in these comparisons to give careful fits to the data by detailed parameter searches. Rather, we are attempting to show the general relationship between elastic and inelastic reactions. The fastidious may therefore find that some of our "fits" are not up to the quality one sometimes finds in more detailed empirical work. Usually those fits require parameter tuning that is not, in general, illuminating. Our purpose here is not to "fit" the data in that sense but rather to try to shed some light on their dynamical content by relating it to other reaction data.

We have developed two ways of looking at the inelastic scattering. We have asymptotic (large qb_0) analytic expressions [Eq. (2.40)] based on ADL and we have the data-to-data formula [Eqs. (2.50) and (2.51)]. We have obtained these data-to-data forms from the analytic expressions, but since most traces of those expressions have disappeared in the final form, it is plausible that the data-to-data expressions have more general validity than their analytic origins imply. That turns out to be the case empirically. We therefore have three questions to investigate: (i) the validity of the asymptotic expressions as approximations to the full amplitude, (ii) the comparison of the approximate expressions with experimental data, and (iii) the validity of the data-to-data forms for relating different experimental quantities. With the single exception of the overall excitation strength λ_L, all input parameters are independently determined. The nuclear density parameters are fixed by electron scattering and the fundamental amplitudes fixed by nucleon-nucleon phase shifts. Thus there remain no adjustable parameters.

We begin with a purely theoretical comparison of the asymptotic approximations and the full amplitude first in a typical light nucleus, oxygen, and then in a heavy nucleus, lead. In Fig. 1 we compare three calculations of the excitation of the 6.13 MeV 3^- state in ^{16}O by 800 MeV protons. The calculation labeled full expression in Fig. 1 is a numerical evaluation based on the full eikonal expression (2.6) using the Tassie transition density (2.7). The excitation strength λ_3 in (2.7) is computed from the measured $B(E3)$,[5] 213 fm,[6] according to Appendix B. In this calculation we use a Fermi density for ^{16}O with parameters taken from electron scattering[6] ($c=2.608$ fm, $\beta=0.513$ fm). For the nucleon-nucleon parameter γ of (2.4) we take $\gamma=2.18+i0.4905$ fm^2 corresponding to a total cross section of $\sigma_T=43.6$ mb and ratio of real to imaginary part $r=-0.225$.[7] The curve labeled Eqs. (2.36) and (2.37) in Fig. 1 is based on the asymptotic amplitudes (2.36) and (2.37) used in (2.35) with G_s of ADL as given in (2.25). All the parameters are as in the full calculation. Finally the curve labeled ASYM is based on the completely asymptotic expression (2.48). We see that away from the forward direction, all three curves have the same shape over six decades. The two asymptotic forms grow together with increasing angle or momentum transfer as we expect since they differ by terms of order $(qb_0)^{-2/3}$. There is a difference in absolute value of at most about 25% between the full and approximate forms, which also decreases with increasing angle. The

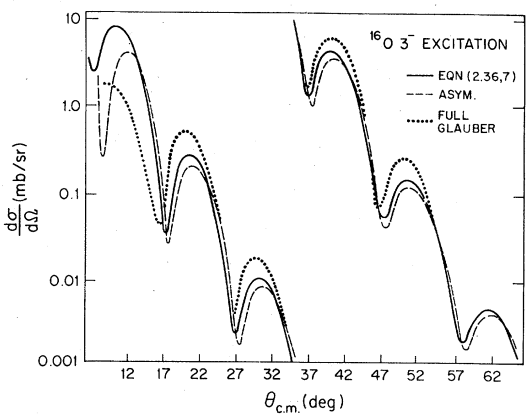

FIG. 1. Comparison of full Glauber (...) [Eq. (2.6)], with the intermediate (——) [Eqs. (2.36) and (2.37)] and asymptotic (---) [Eq. (2.48)] cross section for the excitation of the 6.13 MeV 3^- state in ^{16}O by 800 MeV protons as a function of center of mass angle. The density and interaction parameters are discussed in the text.

difference arises primarily from taking only the leading $(qb_0)^{-1}$ dependence of the $e^{-\gamma\tilde{t}\phi_0}$ term.[8] As shown in ADL, taking the next term [ADL, Eq. (57)] removes the bulk of the discrepancy. However, since we are ultimately aiming at data-to-data relationships which automatically correct for this, we have not included these higher order corrections. The major moral of Fig. 1 therefore is that the asymptotic form converges very rapidly to the Eqs. (2.36) amd (2.37) form and that except at forward angles, and except for a slight difference in scale that is also present for elastic scattering, both forms agree well with the full calculation. The forward angles do not work because our basic approximation at every step has been based on qb_0 large.

In Fig. 2 we show a similar calculation for excitation of the 2.6 MeV 3^- state in Pb by 800 MeV protons. The three curves have the same meaning as in Fig. 1. The excitation strength is again computed from the $B(E3)$,[9] 71400 fm.[6] The parameter is the same as for ^{16}O and the density parameters are fixed by electron scattering[10] $c = 6.6037$ fm, $\beta = 0.6271$ fm. We see again that the asymptotic and Eqs. (2.36) and (2.37) forms do not coincide at small angles but do grow together rapidly with increasing angle. The full expression is again the same in shape but slightly off in absolute scale. That discrepancy also decreases with increasing angle. The variation among the three curves is smaller than for ^{16}O since the radius of ^{208}Pb is larger than that of ^{16}O and qb_0 is the expansion parameter. Once again the moral is that all three forms have generally the same shape, and the asymptotic form converges rapidly to the full amplitude (because of the large radius of Pb). The small scale discrepancy carried over from elastic scattering can be repaired by a more sophisticated treatment of the penetrability factor as in ADL Eq. (57) or by going directly to the data-to-data forms.

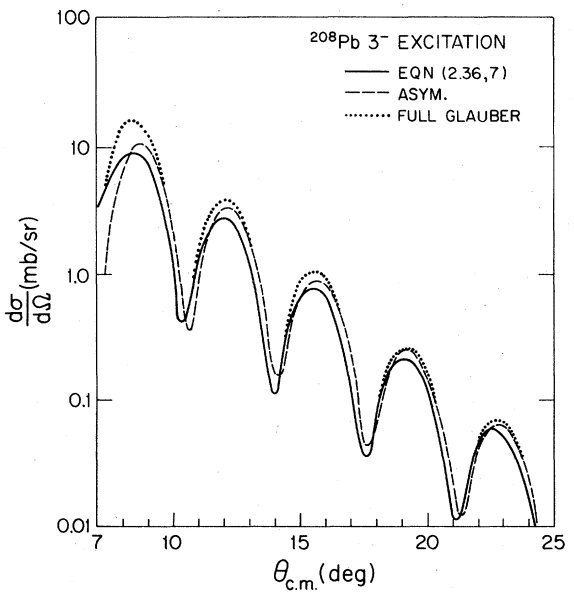

FIG. 2. Same as Fig. 1 but for the 2.6 MeV 3^- state in ^{208}Pb.

We now turn to comparison of the asymptotic forms for the excitation cross section with data. In Fig. 3 we show the cross section for excitation of the 2.6 MeV 3^- and 3.2 MeV 5^- states in ^{208}Pb by 800 MeV protons as a function of angle. The data are from Ref. 11; the curves are from the asymptotic form based on Eq. (2.48). The eikonal parameters are the same as used in Fig. 2. In particular the values of the Fermi density parameters β and c are derived by fitting the pole position in the charge density of ^{208}Pb as deduced from electron scattering by Nagao and Torizuka.[10] We chose to match to the first pole position since the Fermi distribution has been supplanted in these recent analyses of electron scattering from heavy nuclei by a more complicated form, but the work of ADL demonstrates that the principal features of the distribution controlling the shape of the cross section is the pole position. In fixing the overall scale of the cross section in Fig. 3 we have used the connection between λ_L and $B(EL)$ given in Appendix B and we find $B(E3)_{pp'} = 1.6[B(E3)]_{ee'}$ and $B(E5)_{pp'} = 3.2B(E5)_{ee'}$ based on the electro-excitation widths reported in Ref. 9. These fitting factors of 1.6 and 3.2 (uncertain by the 20–25% normalization problem we discussed in connection with Fig. 2) represent dynamical information on the excitation mechanism that we extract from our fit and reflect the added contribution of the neutrons to the hadronic excitation of ^{208}Pb compared with electro-excitation. We note that the fit in Fig. 3 is quite good both as to general trend and details of shape. This is no surprise since we knew that the assumption of distorted waves and surface peaked transition density can fit the data in the far more complex optical model calculations that are traditionally done and we have shown here that our approximations lead to a very adequate representation of that same amplitude.

Our studies thus far have focused on odd L states, but since our formalism treats odd and even L differently, it is interesting to turn to even L. In Figs. 4 and 5 we show the inelastic cross section for excitation of the 1.408 MeV and 2.959 MeV 2^+ states in ^{54}Fe by 800 MeV proton and a function of angle. The data are from Ref. 12. The calculation is again based on the asymptotic form Eq.

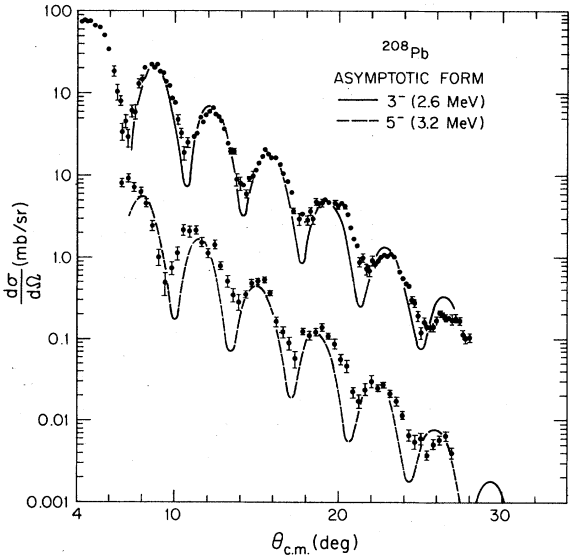

FIG. 3. Cross section for the inelastic excitation of the 3^- (2.6 MeV) state and 5^- (3.2 MeV) state in ^{208}Pb by 800 MeV protons as a function of center of mass angle. The data are from Ref. 11. The calculation is based on the asymptotic amplitude (2.48). The parameters used for the nuclear density, interaction strength, and transition strength are discussed in the text.

(2.48) or for the 2^+ states Eqs. (2.29) and (2.31). For γ we take the same values as for Pb, while the density parameters are taken from electron scattering[13] $c=4.012$ fm, $\beta=0.534$ fm. The overall scale in Fig. 4 was fitted to the data.

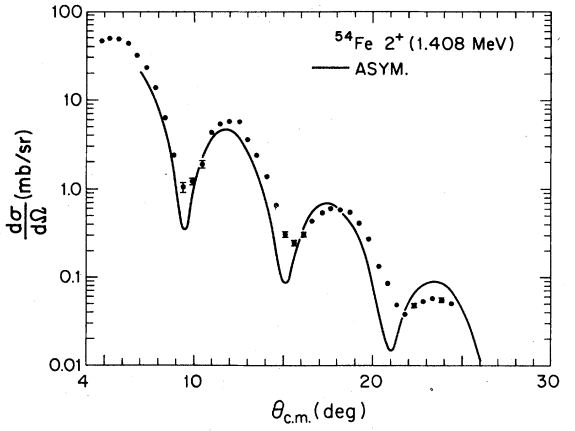

FIG. 4. Cross section for the inelastic excitation of the first 2^+ (1.408 MeV) state in ^{54}Fe by 800 MeV protons as a function of center of mass angle. The data are from Ref. 12. The calculation is based on the asymptotic amplitude (2.48) and the parameters used for the nuclear density, interaction strength, and transition strength are discussed in the text.

Using the results of Appendix B, we find this normalization corresponds to $B(E2)_{pp'}=0.8B(E2)_{ee'}$. Since ^{54}Fe is nearly a $T=0$ nucleus, this is a reasonable result. For the normalization in Fig. 5 we find the ratio $B(E2,\ 2_2^+\rightarrow 0_L^+)/B(E2,\ 2_1^+\rightarrow 0_1^+)=0.4$. Earlier studies[14] using electrons or low energy hadrons obtain ratios between 0.25 and 1.0. This indicates that different probes couple somewhat differently to the inelastic excitation at different energy and momentum transfer, and/or that comparison of excitation strengths is considerably more model dependent that comparisons of shapes. It is certainly clear that the shape is again very well given in Figs. 4 and 5.

Finally we turn to our data-to-data formulas. We examine the same cases as above, ^{208}Pb and ^{54}Fe. In Fig. 6 we show the same ^{208}Pb data as in Fig. 3 for excitation of the 2.6 MeV 3^- and 3.2 MeV 5^- states by 800 MeV protons. The curves are from the data-to-data formula (2.51) with the density parameters β and c needed to make the shift the same as used for Fig. 3. The elastic scattering data are from Ref. 11. The agreement in Fig. 6 is remarkable, even better than that in Fig. 3. This underscores the fact that the slight difficulties in the agreement in Fig. 3 are basically problems in the elastic scattering, not in the excitation, so that in the data-to-data formalism they disappear. The normalization in Fig. 6 obtained by relating λ_L in (2.51) to $B(EL)$ as in Appendix B corresponds to $B(E3)_{pp'}=1.1B(E3)_{ee'}$ and $B(E5)_{pp'}=2.2B(E5)_{ee'}$, again showing the added influence of the neutrons in the hadronic excitation. The discrepancy between the scale factors needed to normalize Figs. 3 and 6 are largely associated with the scale problem in G_s as we discussed, and therefore the factors for Fig. 6 are more reliable. However, the difference we discussed among dif-

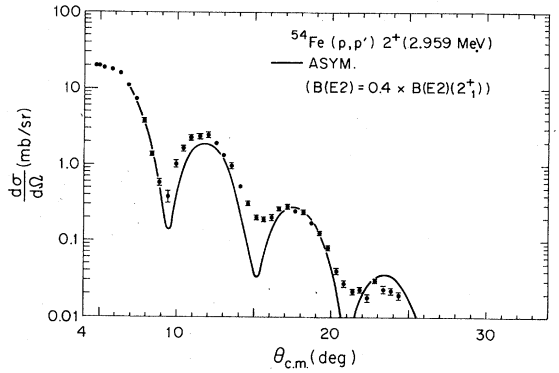

FIG. 5. Same as Fig. 4, but now for the 2.959 MeV 2^+ state in ^{54}Fe.

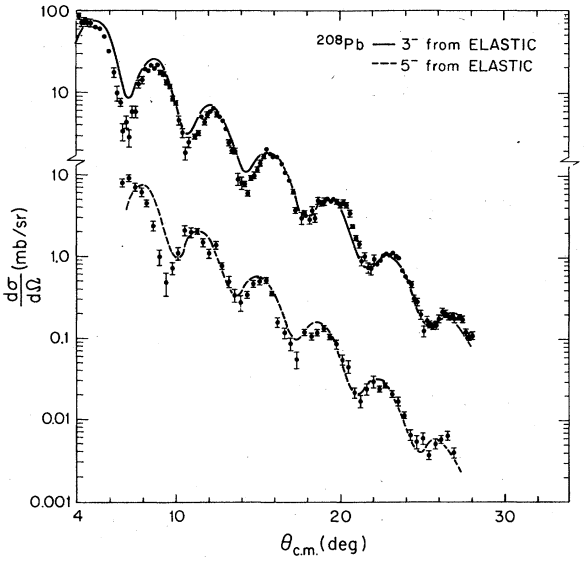

FIG. 6. Cross sections for excitation of the 3^- (2.6 MeV) and 5^- (3.2 MeV) states in ^{208}Pb by 800 MeV protons as a function of center of mass angle. The data are from Ref. 11. The calculation is based on our data-to-data formula (2.51) and used the elastic p-^{208}Pb data of Ref. 11. The nuclear density parameters used in the calculation are obtained from electron scattering as discussed in the text. The vertical normalization is related in the text to the appropriate $B(EL)$.

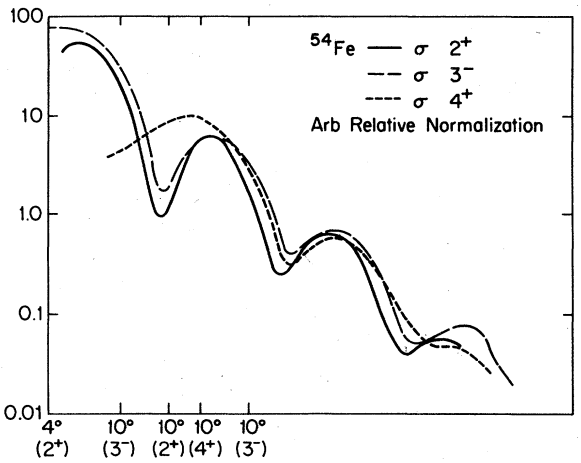

FIG. 7. Smooth curves through the data for the excitation of the 2^+ (1.408 MeV), 3^- (4.782 MeV), and 4^+ (2.538 MeV) states in ^{54}Fe by 800 MeV protons as a function of shifted center of mass angle. The data are from Ref. 12, and the vertical normalization is arbitrary. The angle shifts have been calculated using our data-to-data formula (2.51) and nuclear density parameters taken from electron scattering as discussed in the text. The 3^- appears shifted both to the left and to the right.

ferent reactions in connection with Fig. 5 should indicate that these normalizations are model dependent and should probably not be taken too seriously. In any case they come out to be of the correct order of magnitude, and that plus the striking agreement in shape of Fig. 6 is certainly gratifying.

For ^{54}Fe we have not been able to find any 800 MeV proton elastic scattering data and hence we cannot make a data-to-data comparison directly with (2.51). However in ^{54}Fe, the (p,p') reaction has been studied with 800 MeV protons for the 1.408 MeV 2^+, 4.782 MeV 3^-, and 2.538 MeV 4^+ states.[12] We can use the data-to-data formula (2.51) to compare these with one another. We need only use one 2^+ state since it is clear from Figs. 4 and 5 that both have the same shape. In Fig. 7 we show the data for (p,p') reactions in ^{54}Fe to the first 2^+ state and to the 3^- and 4^+ states plotted with the angle shift corresponding to formula (2.51). The relative normalization is arbitrary, and rather than show the data points directly we show a smooth curve that runs through the data. Since the 3^- can be shifted by $\pm\pi/2$ with respect to the 2^+ and 4^+, we show both the + and − shifts. The density parameters β and c needed to calculate the angle shifts are the same as used in Figs. 4 and 5. The data-to-data formula (2.51) requires that when appropriately shifted, the three inelastic cross sections should coincide, and so they do. We see from Fig. 7 that they do not coincide at very small angles, as they should not, but they heal to agreement rapidly with the highest J taking longest to heal, all as we expect. The agreement between the purely empirical curves in Fig. 7 is further striking evidence for the validity of the data-to-data formula. In fact, one could use the inelastic data in Fig. 7 to reconstruct the elastic data.

We could go on comparing inelastic and elastic data, $B(EL)$'s, etc., but as we mentioned above, that is not our purpose. In fact, for most data available, detailed calculations have already been done with considerable success. These many calculations have been done largely in the context of the optical model, but we have seen that our approximate amplitudes given an excellent representation of those calculations and there is therefore no need to further repeat their agreement. It is only our purpose here to shed some light on the dynamical content of these calculations and, by particularly stressing the data-to-data formula, on their relationship to elastic scattering—a relationship that underscores the geometric origins of the processes. We have seen that our asymptotic formulas reproduce the data's shape and general magnitude except in the forward direction

where our asymptotic approximation is guaranteed to fail. We do not believe that any essential dynamics are hidden in the forward scattering region beyond the obvious threshold factors. We have also seen that the data-to-data formulas do an even better job of fitting the details of the data and also remove some inadequacies in the simple asymptotic form. The close connection we find between electron and hadron excitation strengths depends on the full density distribution as shown in Appendix B and therefore the connection between $B(EL)_{pp'}$ and $B(EL)_{ee'}$ is model dependent and should be read with restraint.

Finally there is the very interesting question of corrections to the reaction mechanism or transition density. Assuming it to be local makes the formalism questionable for two-step processes such as pion double charge exchange and perhaps even pion resonant scattering, although preliminary indications are that the data-to-data formulas will work even there. In general it is not clear how the formalism could be extended to deal with nonlocality. The surface or Tassie form of Eq. (2.7) is the other assumption we make. This seems to be a detailed dynamical assumption, but in fact, strong absorption and refraction will concentrate the excitation mechanism at the surface, no matter what the detailed form of the transition density and it is just this surface dominance that our asymptotic method exploits. Since for (p,p') reactions at medium energy the absorption and refraction are strong, it may be difficult to distinguish excitation mechanisms in these reactions. It is the surface nature of the reaction that gives it such a strong geometric quality and hence relates it so closely to elastic scattering. The geometric enhancement of a Tassie-type transition density indicates that probing differences between the Tassie and other microscopic forms may prove quite difficult with protons. It would be interesting to apply these methods to less strongly interacting probes as a better test of the reaction mechanism.

It should be noted that the formalism developed in this paper could easily be extended to reactions involving targets with spin.

IV. DISCUSSION

We have studied inelastic scattering of hadrons by nuclei at intermediate energies. The basic input of the theory of these reactions is the distorted wave impulse approximation and some simple model of the transition density for the inelastic scattering. At intermediate energies it is reasonable to treat the distortion in the eikonal approximation, and our work on these reactions therefore becomes an extension of our recent work on elastic hadron-nucleus scattering in the eikonal approximation (ADL).

Just these theoretical ingredients or, equivalently, the optical model have been used by many others in detailed calculations applied to the large body of excellent data. These are normally complicated numerical calculations that must be done with considerable care because the large wave numbers involved lead to rapidly oscillating functions and much cancellation. The results of these calculations usually agree quite well with the data. The data all share oscillations in momentum transfer that is characteristic of diffraction scattering superimposed on a univeral exponential falloff. These features suggest a unified geometric origin for all the processes, but that unified view is difficult to see through complicated numerical calculations.

In this paper we have attempted to make a direct analytic evaluation of the relevant reaction amplitudes. With simple models for the transition density, exploiting refraction and absorption of the probe and using the asymptotic models of ADL, we can obtain closed form analytic expressions for the relevant amplitudes. These work well when compared with experiment but, better still, they permit the inelastic cross sections to be expressed directly in terms of the elastic cross section, using no adjustable parameters, apart from an overall strength. This overall strength can in part be related to the electromagnetic $B(EL)$. The data-to-data formula (2.51) works remarkably well in inter-relating inelastic and elastic cross sections as was shown in Sec. III. The major dynamical input in this relation is the local, surface peaked nature of the transition density. Locality may limit these results to one-step processes, perhaps even ruling out application to resonant pion scattering, but we hope that the dominance of nuclear geometry and the simplicity of the final formulas may lead to useful insights even for pion reactions. The assumption of surface peaking is probably less significant dynamically so long as we are dealing with strongly interacting and absorbed probes, since both the strong absorption and strong refraction forces the inelastic interaction to occur at the surface whether the transition density peaks there or not. This feature will probably permit application to pions. To study the details of the transition density it would seem profitable to turn to less strongly interacting probes such as electrons, K mesons, or the like. We plan to do just that.

A remarkable feature of the data-to-data formulas is that they bear little trace of the assump-

tions used to derive them since they basically simply relate cross section to cross section. This makes plausible far wider application of the result than the original derivation seems to permit. We have already seen that the data-to-data formulas more correctly include details of the dynamics than their simple asymptotic origins and we hope to be able to extend that use to other inelastic reactions involving particle transfer, inclusive processes, etc.

In summary, nuclear excitation with protons and other strongly interacting probes seems to depend primarily on the nuclear geometry. By using the geometry of the nucleus, and its concomitant analytically, we can evaluate the integrals for the amplitudes by asymptotic methods that exploit the very features of rapid oscillation that makes direct numerical evaluation so difficult. To the extent, then, that our asymptotic expansion is valid, our forms are equivalent to the detailed numerical evaluation.

What does all this teach us? At medium energies, elastic and simple inelastic scattering with strongly interacting probes are dominated by nuclear geometry and the inelastic coupling strengths. Reaction mechanisms or details of nuclear structure are therefore difficult to study in this way. These are more clearly manifested in more complicated inelastic processes, e.g., two-step processes, or in the scattering of less strongly absorbed probes. We plan to turn our attention to these problems. Meanwhile we can continue to be pleasantly surprised by the power of the eikonal approximation to describe and correlate a wide range of nuclear data, and in particular of the simple form and impressive success of the data-to-data expressions.

ACKNOWLEDGMENTS

The authors are grateful to Dr. Stephen Barr for providing a derivation of Eq. (2.50), and to Professor S. Wallace for providing the nucleon-nucleon amplitudes based on the Arndt analysis. Three of us (R.D.A., J.A.M., D.A.S.) were partially supported by a grant from the U. S. National Science Foundation.

APPENDIX A

In this appendix we show that the step from Eq. (2.42) to (2.43) is justified. Consider the integral in (2.42)

$$\int_0^\infty db\, b^{L-2n+1} J_M(qb) e^{-\chi(b)} \times \int_{-\infty}^{\infty} dz\, z^{2n-1} \frac{d}{dz} \rho[(z^2+b^2)^{1/2}], \tag{A1}$$

where we have used $(1/r)(d/dr) = (1/z)(d/dz)$ to transform the inner integral. Integrating once by parts we have

$$\int_0^\infty db\, b^{L-2n+1} J_M(qb) e^{-\chi(b)} (2n-1) \times \int_{-\infty}^{\infty} dz\, z^{2n-2} \rho[(z^2+b^2)^{1/2}]. \tag{A2}$$

We evaluate the inner integral in the spirit of ADL, taking only the part singular near b_0. The singular part of the density is

$$\rho_s = \frac{-2b_0\beta\rho_0}{z^2+b^2-b_0^2}. \tag{A3}$$

Strictly putting ρ_s in the inner integral of (A2) leads to an improper integral, but of course the true density leads to a convergent integral and we are only concerned with the contribution to the integral near the singularity. We can therefore be cavalier about the evaluation. We write

$$\int_{-\infty}^{\infty} dz\, z^{2n-2} \rho_s = -2b_0\beta\rho_0 \left(\frac{1}{i}\frac{\partial}{\partial\eta}\right)^{2n-2} \times \int_{-\infty}^{\infty} \frac{e^{i\eta z} d_z}{z^2+b^2-b_0^2}, \tag{A4}$$

where we set $\eta = 0$ after evaluating the integral. (A4) gives

$$-2\beta\rho_0 b_0 \pi \left(\frac{1}{i}\right)^{2n-2} (b^2-b_0^2)^{n-3/2}. \tag{A5}$$

We substitute this in (A2) and evaluate the integral as in ADL. There it is shown that the stationary phase point is $b = b_s$ and all other b dependence can be evaluated at b_s. ADL write

$$b_s = b_0 + \delta, \tag{A6}$$

and find

$$\delta = -\frac{b_0}{2}\left(-\frac{\alpha}{qb_0}\right)^{2/3},$$

so that

$$(b^2-b_0^2) \cong (b_s^2-b_0^2) = -b_0^2\left(-\frac{\alpha}{qb_0}\right)^{2/3}. \tag{A7}$$

The integral in (A2) becomes

$$-2\beta\rho_0\left(-\frac{\alpha}{qb_0}\right)^{2/3(n-1)-1/3} (2n-1) \int_0^\infty b\, db\, J_M(qb) e^{-\chi(b)}. \tag{A8}$$

The $n=0$ case is dealt with explicitly in the text. We see that even $n=1$ is $\sim(qb_0/\alpha)^{1/3}$ compared with (qb_0) of the $n=0$ term, and higher terms are down by $(qb_0/\alpha)^{-2/3}$ for each power of n.

APPENDIX B

In this appendix we derive a relationship between the electromagnetic $B(EL)$ and the inelastic transition strength in the Tassie model. We write

$$f_L = \lambda_L r^L \frac{1}{r}\frac{d}{dr}\rho(r) . \tag{B1}$$

We assume that we may factor λ_L into an overall strength, related to the hadron-nucleon total cross section and a nuclear structure strength, C_L to be related to the $B(EL)$

$$f_L = \gamma C_L r^L \frac{1}{r}\frac{d}{dr}\rho(r) = \gamma \rho_{tr}(r) . \tag{B2}$$

This factorization is best if the hadron-nucleon t matrix and the proton-charge form factor are both slowly varying compared with the nuclear form factor (alternatively the interaction range is short compared with the nuclear size). If this is the case and if we may treat protons and neutrons as equivalent, the transition densities for hadron and electromagnetic processes are simply related. The $B(EL)$ may be expressed in terms of the transition density as

$$B(EL)\uparrow = 4\pi |\langle L \| Y_L \| 0\rangle|^2 |\langle r^L \rho_{tr}\rangle|^2 . \tag{B3}$$

The factor of 4π appears in (B3) because the initial state angular function $Y_{00} = (4\pi)^{-1/2}$ was incorporated into f_L in Eq. (2.5), but appears explicitly in the angular matrix element here. Evaluating the angular matrix element gives

$$\begin{aligned} B(EL)\uparrow &= (2L+1)^2 \begin{pmatrix} L & L & 0 \\ 0 & 0 & 0 \end{pmatrix}^2 |\langle r^L \rho_{tr}\rangle|^2 \\ &= (2L+1)|\langle r^L \rho_{tr}\rangle|^2 . \end{aligned} \tag{B4}$$

For the radial integral we have

$$\begin{aligned} \langle r^L \rho_{tr}\rangle &= C_L \int_0^\infty r^L \left(r^L \frac{1}{r}\frac{d\rho}{dr}\right) r^2 dr \\ &= C_L \int_0^\infty r^{2L+1} \frac{d\rho}{dr} d_r \\ &= -C_L (2L+1) \int_0^\infty r^{2L} \rho(r) dr . \end{aligned} \tag{B5}$$

So our general result is

$$B(EL)\uparrow = (2L+1)^3 C_L{}^2 \left[\int_0^\infty r^{2L}\rho(r) dr\right]^2 , \tag{B6}$$

where ρ is normalized to Z for electromagnetic applications [e.g., (e, e')] and to A for hadronic applications [e.g., (p, p')] in order to have the same C_L in both cases.

For the special case of a Fermi distribution

$$\begin{aligned} \rho(r) &= \rho_0 \{1 + \exp[(r-c)/\beta]\}^{-1} , \\ \rho_0 &= \frac{z}{4\pi}\left(\int_0^\infty r^2 dr \{1 + \exp[(r-c)/\beta]\}^{-1}\right)^{-1} . \end{aligned} \tag{B7}$$

The integrals are all of the form

$$I_{2m} = \int_0^\infty dr\, r^{2m} \{1 + \exp[(r-c)/\beta]\}^{-1} ,$$

which may be evaluated analytically to give

$$\begin{aligned} I_{2m} = \frac{c^{2m+1}}{2m+1}\left[1 + 2\sum_{s=1}^{m} \epsilon^s \frac{(m+1)!\,(2^{2s-1}-1)}{(2m-2s+1)!\,(2s)!} |B_{2s}|\right] \\ + \beta^{2m+1}(2m)! \sum_{k=1}^{\infty} (-1)^{k+1} \frac{e^{-kc/\beta}}{k^{2m+1}} , \end{aligned} \tag{B8}$$

where B_{2s} are Bernoulli numbers, and $\epsilon = (\pi\beta/c)^2$. Using Eq. (B8) in Eq. (B6) we obtain

$$B(EL)\uparrow = (2L+1)^3 (C_L)^2 \left(\frac{Z}{4\pi}\right)^2 \left(\frac{I_{2L}}{I_2}\right)^2 . \tag{B9}$$

We see trivially that for $L = 1$ the nuclear structure integrals divide out. For higher L neglecting the exponential terms $e^{-c/\beta}$ (an excellent approximation even for p-shell nuclei) enables one to write

$$\frac{I_{2L}}{I_2} = \frac{3c^{2L-2}}{2L+1} P_{(L)}(\epsilon) . \tag{B10}$$

$P_{(L)}(\epsilon)$ is a $(L-1)$ order polynomial in ϵ determined from (B8), and defined such that $P_{(L)}(0) = 1$ for all L. (Note that these $P_{(L)}$'s are *not* the Legendre polynomials.) We then have

$$B(EL)\uparrow = (2L+1)\left(\frac{3Z}{4\pi}\right)^2 c^{4(L-1)} C_L{}^2 [P_{(L)}(\epsilon)]^2 \tag{B11}$$

or

$$C_L = \left(\frac{B(EL)\uparrow}{2L+1}\right)^{1/2} \frac{4\pi}{3Zc^{2(L-1)}} [P_{(L)}(\epsilon)]^{-1} . \tag{B12}$$

These are the relations used to normalize the cross sections. The polynomials $P_{(L)}$ for the case of a Fermi distribution are given in Eq. (B13)

$$\begin{aligned} P_{(1)} &= 1 \\ P_{(2)} &= 1 + \tfrac{7}{3}\epsilon \\ P_{(3)} &= 1 + 6\epsilon + \tfrac{31}{3}\epsilon^2 \\ P_{(4)} &= 1 + 11\epsilon + \tfrac{239}{5}\epsilon^2 + \tfrac{381}{5}\epsilon^3 \\ P_{(5)} &= 1 + \tfrac{52}{3}\epsilon + \tfrac{410}{3}\epsilon^2 + \tfrac{1636}{3}\epsilon^3 + \tfrac{2555}{3}\epsilon^4 . \end{aligned} \tag{B13}$$

*Permanent address: SIN, Villigen CH5234, Switzerland.

[1]R. D. Amado, J.-P. Dedonder, and F. Lenz, Phys. Rev. C 21, 647 (1980). (ADL in this work.)

[2]L. J. Tassie, Aust. J. Phys. 9, 407 (1956).

[3]J. S. Blair, Phys. Rev. 115, 928 (1959); J. S. Blair, *Lectures in Theoretical Physics* VIII C, edited by P. D. Kunz, D. A. Lind, and W. E. Brittin (University of Colorado Press, Boulder, 1966).

[4]There is earlier work in a different context that attempts to relate elastic and inelastic scattering [cf., N. Austern and J. S. Blair, Ann. Phys. (N.Y.) 33, 15 (1965)].

[5]F. Ajzenberg-Selove, Nucl. Phys. A281, 1 (1977).

[6]I. Sick and J. S. McCarthy, Nucl. Phys. A150, 631 (1970).

[7]These are typical values, but for r there is considerable variation in the literature. Compare Ref. 16.

[8]There is a misprint in the expansion coefficients for $\tilde{t}(b_0)$ given in ADL Appendix A. Equations (A4b) and (A4c) of ADL should read $a_2=-0.980$ and $a_3=0.157$, respectively. We have checked by direct numerical evaluation of the integral that, for all cases of interest to us, expansion through the $a_3 r^3$ term in ADL Eq. (A3) is completely adequate.

[9]J. F. Ziegler and G. A. Peterson, Phys. Rev. 165, 1337 (1968).

[10]M. Nagao and Y. Torizuka, Phys. Lett. 37B, 383 (1971).

[11]G. S. Blanpied *et al.*, Phys. Rev. C 18, 1436 (1978).

[12]G. S. Adams *et al.*, Phys. Rev. C 21, 2485 (1980).

[13]A. S. Litvinenko *et al.*, Yad. Fiz. 14, 40 (1971) [Sov. J. Nucl. Phys. 14, 23 (1972)].

[14]H. Verheul and R. D. Auble, Nucl. Data Sheets 23, 455 (1978).